Project	**IEEE 802.16 Broadband Wireless Access Working Group <http://ieee802.org/16>**
Title	**Symmetric UL/DL diversity permutations for OFDMA PHY**
Date Submitted	**2005-1-27**

Source(s)	Ran Yaniv, Tal Kaitz, Vladimir Yanover, Naftali Chayat, Kfir Blum, Yoni Dallal, Danny Stopler **Alvarion Ltd.**	ran.yaniv@alvarion.com tal.kaitz@alvarion.com
	InSeok Hwang, Jaehee Cho, Soonyoung Yoon **Samsung Electronics, Inc.**	
	Yuval Lomnitz **Intel**	
	Dave Pechner, Todd Chauvin, Doug C. Dahlby **ArrayComm**	
	Bin-Chul Ihm, Yongseok Jin, Jinyoung Chun, Kyuhyuk Chung **LG Electronics, Inc.**	

Re:	Call for contributions, IEEE P802.16e/D5 Sponsor Ballot
Abstract	
Purpose	
Notice	This document has been prepared to assist IEEE 802.16. It is offered as a basis for discussion and is not binding on the contributing individual(s) or organization(s). The material in this document is subject to change in form and content after further study. The contributor(s) reserve(s) the right to add, amend or withdraw material contained herein.
Release	The contributor grants a free, irrevocable license to the IEEE to incorporate material contained in this contribution, and any modifications thereof, in the creation of an IEEE Standards publication; to copyright in the IEEE's name any IEEE Standards publication even though it may include portions of this contribution; and at the IEEE's sole discretion to permit others to reproduce in whole or in part the resulting IEEE Standards publication. The contributor also acknowledges and accepts that this contribution may be made public by IEEE 802.16.
Patent Policy and Procedures	The contributor is familiar with the IEEE 802.16 Patent Policy and Procedures <http://ieee802.org/16/ipr/patents/policy.html>, including the statement "IEEE standards may include the known use of patent(s), including patent applications, provided the IEEE receives assurance from the patent holder or applicant with respect to patents essential for compliance with both mandatory and optional portions of the standard." Early disclosure to the Working Group of patent information that might be relevant to the standard is essential to reduce the possibility for delays in the development process and increase the likelihood that the draft publication will be approved for publication. Please notify the Chair <mailto:chair@wirelessman.org> as early as possible, in written or electronic form, if patented technology (or technology under patent application) might be incorporated into a draft standard being developed within the IEEE 802.16 Working Group. The Chair will disclose this notification via the IEEE 802.16 web site <http://ieee802.org/16/ipr/patents/notices>.

Symmetric UL/DL diversity permutations for OFDMA PHY

Ran Yaniv, Tal Kaitz, Naftali Chayat, Vladimir Yanover, Kfir Blum, Yoni Dallal, Danny Stopler

Alvarion Ltd.

1 Introduction

The objective of this contribution is to introduce downlink permutation schemes that are symmetric to the uplink PUSC permutation schemes currently defined. The motivation is to enable optimal adaptive beamforming through pairing of UL and DL allocations while maintaining the desired properties of uplink PUSC structures, namely frequency diversity and cell-based tile permutations.

The contribution is organized as follows. The performance aspects of the proposed changes are elaborated upon in the next section, followed by an outline of the proposed solution. Detailed text changes are presented in section 4.

2 Performance aspects of the proposed changes

We consider the major performance improvements associated with the proposed changes. These can be categorized as follows:

Improved interference estimation capabilities.
Due to the tile structure the interference level per tile can be estimated. This improves significantly the performance in CCI conditions.

Improved Interference rejection via OFDMA permuation for beamforming
Currently no scheme is capable of fully exploiting the OFDMA permutation in conjunction with beamforming.

Improved frequency Diversity with beamforming
Frequency diversity is crucial even when spatial diversity is present. The proposed mode provides frequency diversity of order 6 or more.

2.1 Improved interference estimation capabilities.

Let us examine the effect of interference knowledge (or lack thereof) on the link performance in "frequency reuse 1" scenarios where significant co-channel interference is present. It has been previously noted that lack of knowledge at the receiver on the interference level per subcarrier results in severe performance degradation in OFDMA systems that utilize interference-averaging permutations in conjunction with downlink power control [9], [10].

As a test case, we consider a sectorized "universal reuse" deployment in which the same center frequency is reused throughout the system and inter-sector interference is averaged through the use of per-sector subcarrier permutations. Each sector utilizes 50% of its subchannels in order to further inter-sector interference. The MSS of interest is allocated ¼ of the utilized subchannels in its sector (1/8 of the total bandwidth). The interfering BSs divide their active subchannels between 4 different MSSs, and each allocation is transmitted with a different level of power boost resulting from downlink power control.

Two scenarios were examined:

- Scenario A: the MSS of interest is located on the border between 2 sectors; Interference from one other BS is spread over the subcarriers used by the MSS.
- Scenario B: the MSS of interest is located on the border between 3 sectors; Interference from two BSs is spread over the subcarriers used by the MSS.

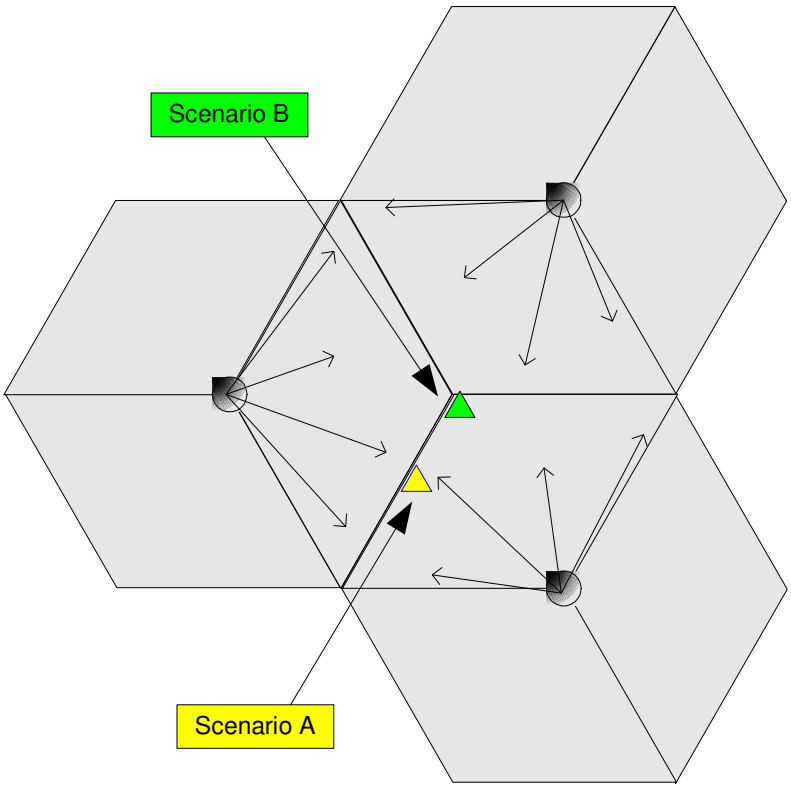

Figure 1 – Sectorized reuse-1 deployment scenario

For both scenarios, the FUSC and the proposed TUSC permutations were examined. While the FUSC permutation does not permit interference estimation per subcarrier, it is interesting to observe the potential gain in the decoding process that such knowledge could provide. With the TUSC tile-based permutation, interference level is more or less constant over a tile, allowing for estimation of the average tile interference using various methods.

The following subsections outline the simulation parameters and results.

2.1.1 Simulation Parameters

The simulation parameters for both scenarios are outlined in the following table:

Parameter	**FUSC**	**TUSC**
FFT length	1024	
Bandwidth	10 MHz	
Center frequency	2.4 GHz	
Packet length	120 bytes	
Modulation and code rate	QPSK ½	
S/N_0	15dB	
Channel model	ITU Vehicular-A, 20km/h velocity, Power from desired BS normalized to unity; Power from interfering BSs governed by the fast fading process.	
FEC	Convolutional Turbo Code; Depending on interference knowledge, LLR metrics were adapted either to the interference level or to white noise.	
Channel estimation	Ideal	
Interference estimation	None / Ideal	
# subchannels for desired MSS's burst	2	4
# subchannels in each burst from interfering BS	2, 2, 2, 2	4, 4, 4, 5
Relative power boost of each burst from interfering BS	0dB, -3dB, -6dB, -9dB	0dB, -3dB, -6dB, -9dB

2.1.2 Simulation results: Scenario A

The MSS of interest in scenario A observes interference from one interfering BS transmitting multiple bursts; both BSs are 50% loaded.

Figure 1 depicts the observed packet error rate vs. SINR. SINR was calculated as the desired signal power divided by the sum of thermal noise and interference power (not accounting for instantaneous fast fading – i.e. assuming all fast fading has been averaged out) seen at the

subcarriers of the desired MSS's allocation. The performance when no interference is present (i.e. the AWGN case) is depicted in the figure for reference.

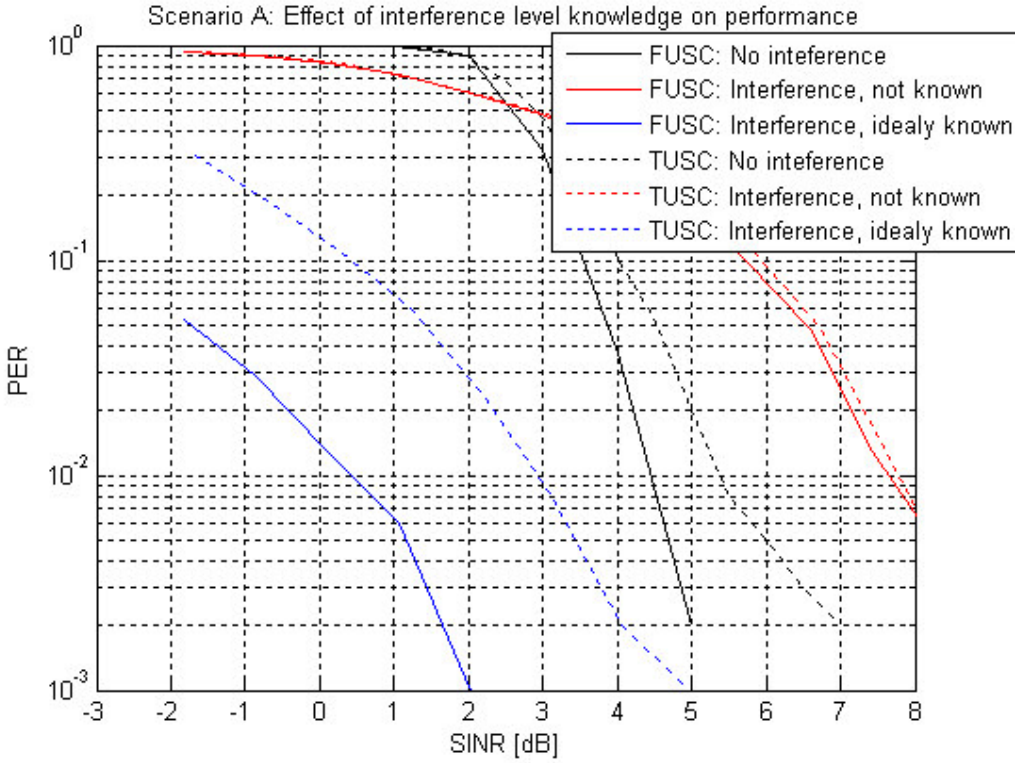

Figure 2 – PER performance for scenario A

As can be observed, the TUSC tile-based permutation with interference knowledge at the receiver outperforms the FUSC permutation without such knowledge by more than 4.5dB and 5dB for outage probabilities of 1% and 10%, respectively. It is interesting to note that the strength of the FUSC permutation only comes into play when interference is known at the receiver. When interference is not known, FUSC does not differ from tile-based schemes.

2.1.3 Simulation results: Scenario B

The MSS of interest in scenario B observes interference from two interfering BSs transmitting multiple bursts; All three BSs are 50% loaded.

Figure 2 depicts the observed packet error rate vs. SINR.

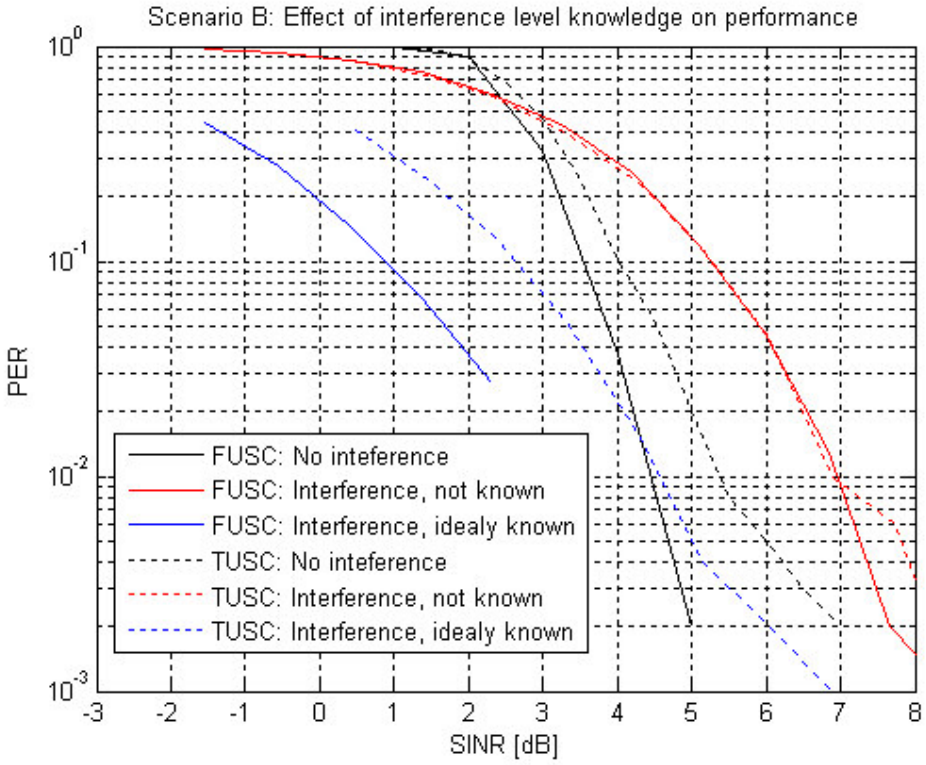

Figure 3 - PER performance for scenario B

In this scenario, the TUSC tile-based permutation with interference knowledge at the receiver still outperforms the FUSC permutation without such knowledge by 2.5dB for outage probabilities of both 1% and 10%.

2.2 Interference reduction via OFDMA permutations in conjunction with beamforming

The following section demonstrates the benefits of the proposed tile based permutation for DL beam forming applications. These benefits are related to the use of OFDMA permutation in conjunction with beamforming.
To demonstrate let us consider a cellular system and let us focus on a specific user in a given cell. When the user is transmitted to, the BS forms a beam towards it. The same operation is also performed in adjacent cells towards other cells. As a consequence, for the major part of the time the desired use is not illuminated by adjacent BSs. However, for a small fraction of the time, the desired user is illuminated by the other BSs.
The performance can be improved by using a tile structure. A tile is a contiguous group of subcarriers. Let us assume that the transmission occurs over K tiles. The assignment of tiles to subchannels is governed by a permutation formula, and the IDcell parameter. Since the adjacent BSs use different cell IDs, the mapping of tiles to subchannels will be different from cell to cell. As a consequence, only a fraction of the tiles will be illuminated by interference. Since the FEC operates over several tiles, the effective interference will be reduced.

Currently none of the modes supporting beamforming fully exploits the interference reduction capabilities of the OFDMA permutations. In FUSC mode beamforming can be performed only over the entire BW. In AMC modes, beamforming can be performed over a single group of contiguous subcarriers, and there is no permutation to reduce interference. In PUSC, beamforming can be performed over major groups. Thus the number of subchannels is small.

In the following we show the performance improvement of a beamforming system as a function of the permutation parameter K, which is defined as the number of subchannels in an adjacent cell that interfere with a single subchannel in the desired cell.

2.2.1 Simulation methodology

The simulation is performed as follows:

- The network is laid out by placing cells on a hexagonal grid and by dividing the cells into sectors.
- The simulation is performed in blocks. Within each block the following operations are performed:
    - Users are placed randomly on the network.
    - Log normal shadowing is generated.
    - Users are assigned to the best BS according to lowest path loss and shadowing.
    - Power control is set.
- A block of simulation is composed of many drops. Each drop corresponds to a transmission to a single or several users. In each drop, the following operations are performed:
    - Users are selected in the desired and other cells.
    - Beamforming is applied towards the users
    - CINR values per tile are computed.
- CINR values are converted to effective CINR using EESM techniques. [8]

- The effective CINR values are used to determine the effective MCS per modulation. When the CINR values are lower than that of the lowest supported MCS the user is declared in outage.
- Effective CINR values per
- The aggregate capacity is computed as the harmonic average of the rates. This is related to fairness criteria based on equal bit-rate to all users. (In contrast to equal air-time).

2.2.2 Simulation parameters

The following simulation parameters were used:

- Path loss exponent of 3.8
- Correlated Lognormal shadowing with sigma=7dB. Correlated shadowing between different BSs to a specific MSS. Un correlated Shadowing between a specific BS to different MSSs.
- Laplacian power azimuth spectrum of 5 degrees. (See [7]).
- Quasi-static channels.
- Convolutional code.
- No power control.
- Interference limited case. The transmit power was set for an average SNR of 20dB at the cell edge.

The following antenna arrays were tested:
ULA4d10 – 4 elements Uniform Linear Array with 10 wavelengths inter-element separation.
Ant1 – single element antenna. Antenna pattern was set according to [7].

2.2.3 Simulation results

Table 1and Table 2 summarize the coverage and capacity results with two extreme values of K and for various deployment and array types. Figure 4 and Figure 5 shows the results as a function of K. The results indicate capacity improvement of up 30% for reuse 3 and 63% for reuse 1.
As can be observed, averaging performance saturates at high K. Saturation region begins at above K~15 for reuse 3, and about K~22 for reuse 1.

Coverage [%]		
System	**K=1**	**K=20**
ULA4d10 reuse1	99.87	100.00
ULA4d10 reuse3	100.00	100.00
Ant1 reuse1	43.43	96.09
Ant1 reuse3	91.29	99.75

Table 1 Coverage results for K=1 K=20

Spectral Efficiency [bps/Hz/Cell]		
System	**K=1**	**K=20**
ULA4d10 reuse1	1.92	3.13

ULA4d10 reuse3	1.96	2.59
Ant1 reuse1	0.87	1.06
Ant1 reuse3	0.50	0.90

Table 2 Spectral efficiency results for K=1 K=20

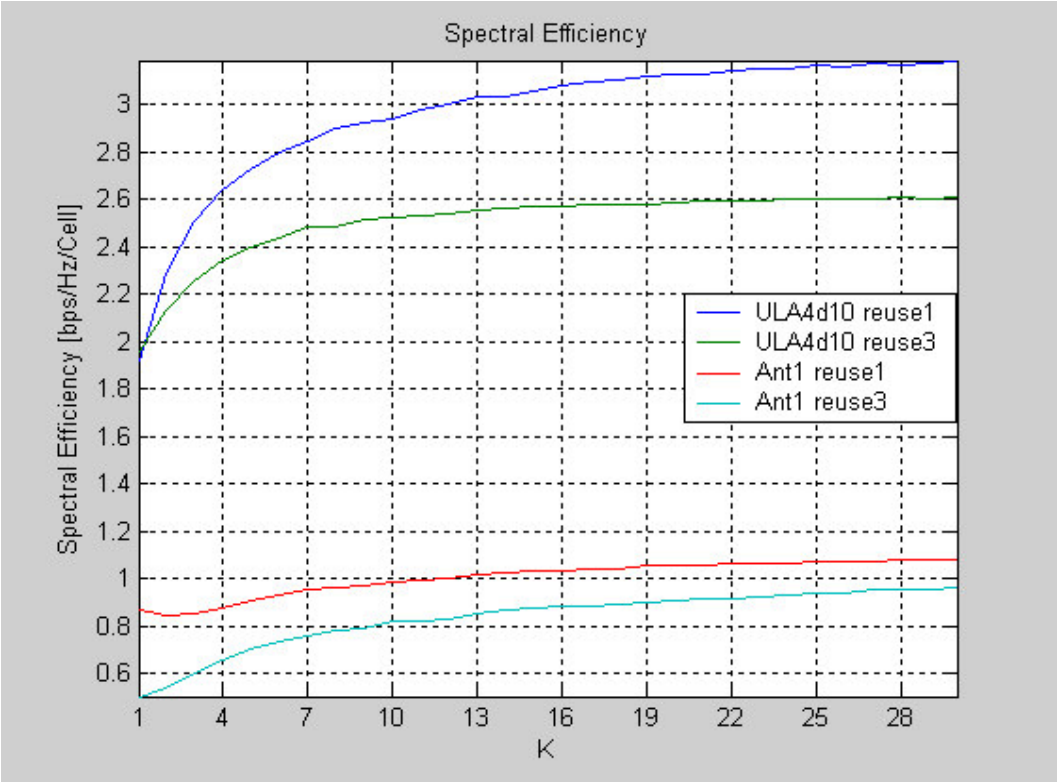

Figure 4 Spectral efficiency as a function of K

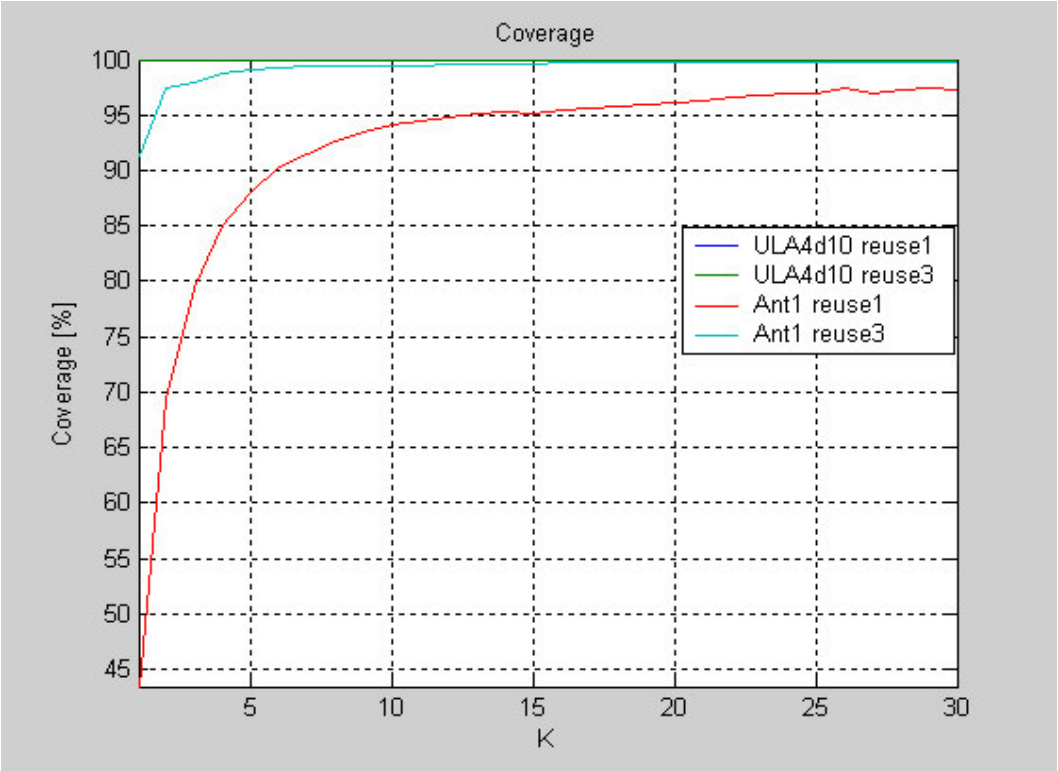

Figure 5 Coverage as a function of K

2.2.3.1 ULA 4 reuse 1 results (K=1)

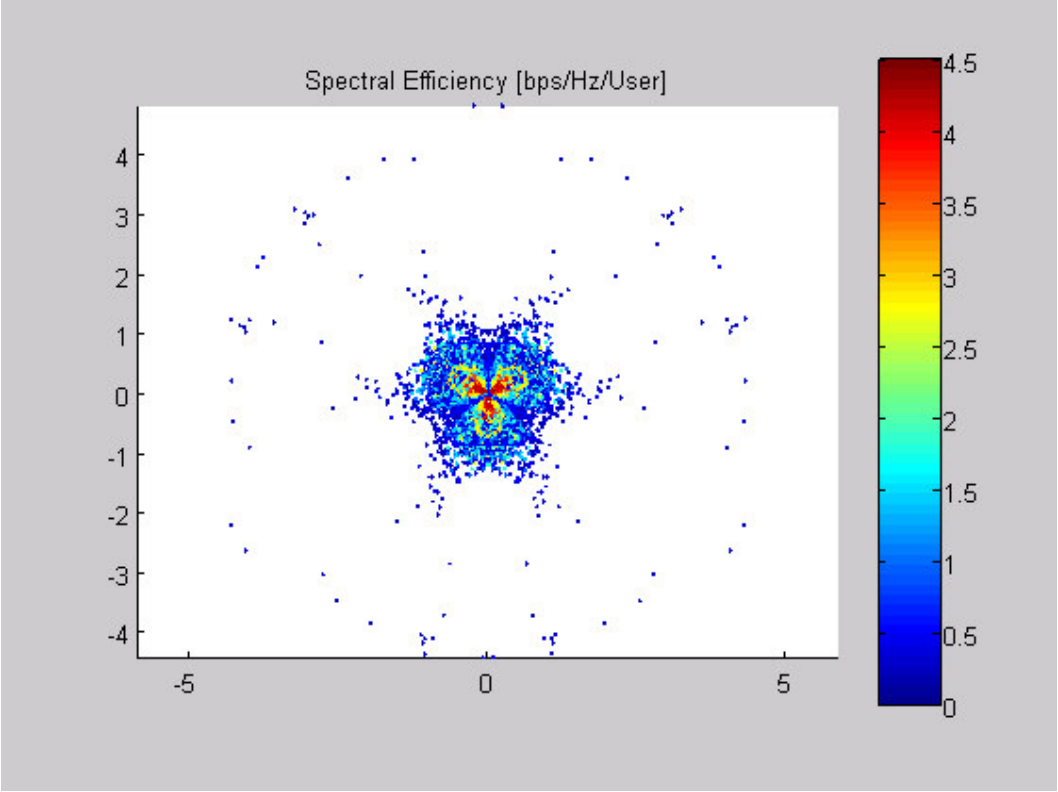

Figure 6

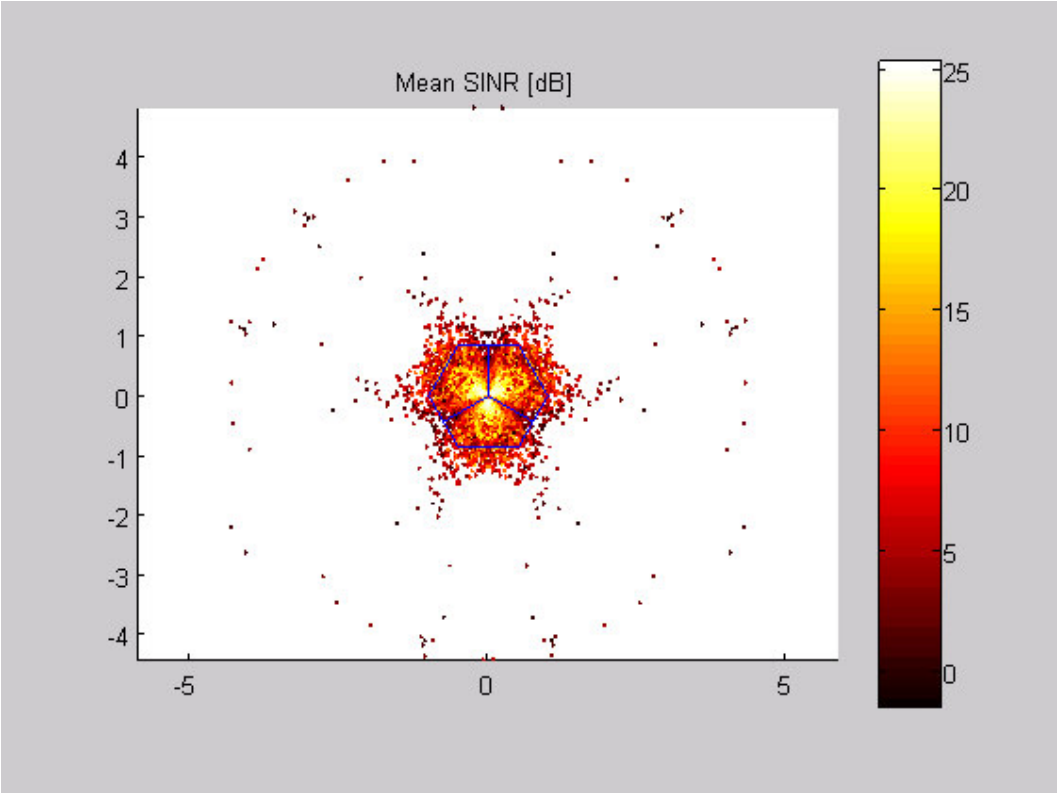

Figure 7

2.2.3.2 ULA 4 reuse 3 results (K=1)

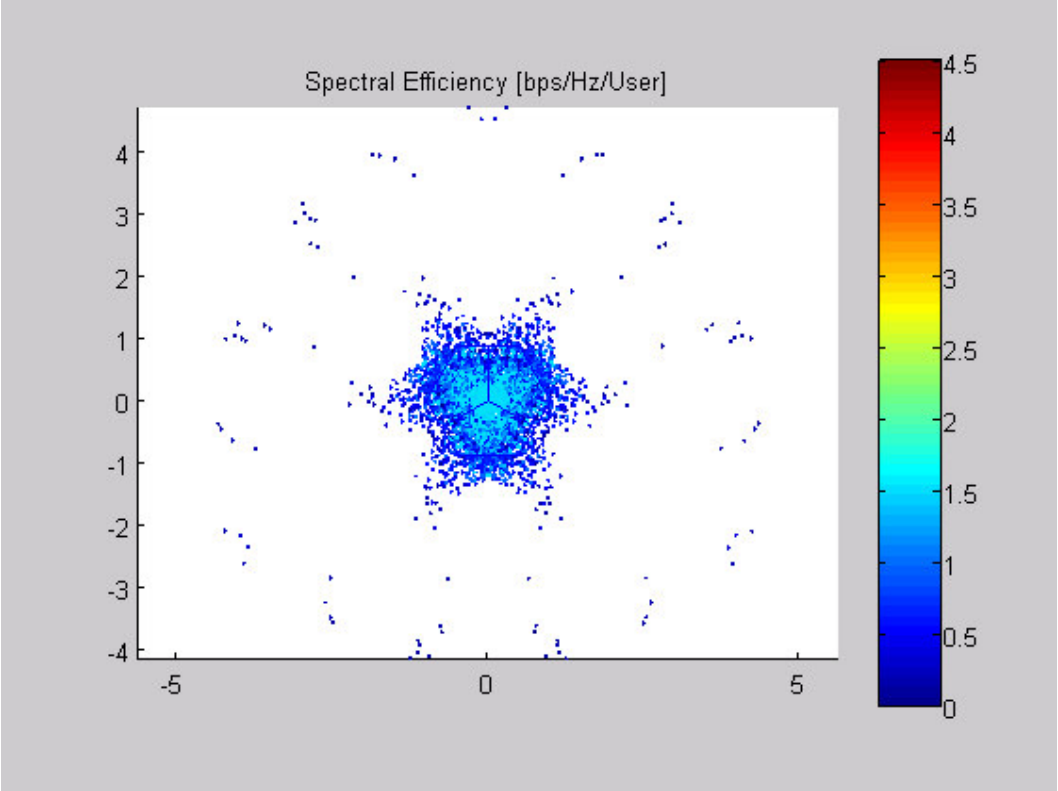

Figure 8

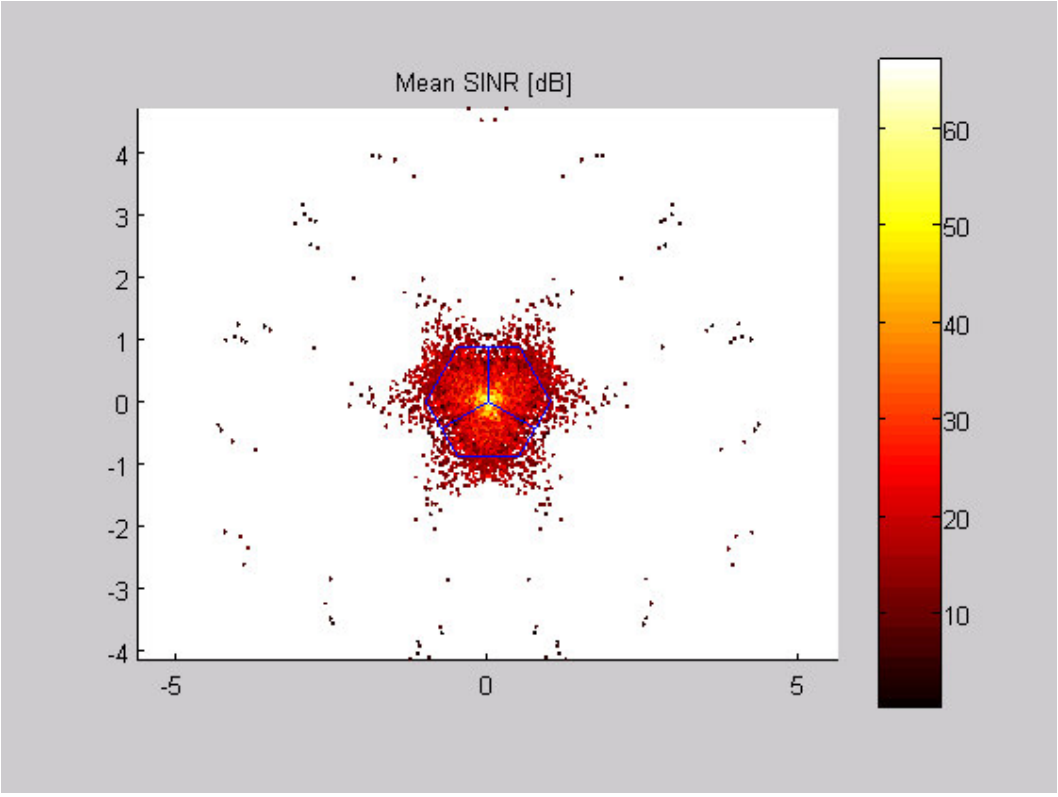

Figure 9

2.2.3.3 Ant1 reuse 1 results (K=1)

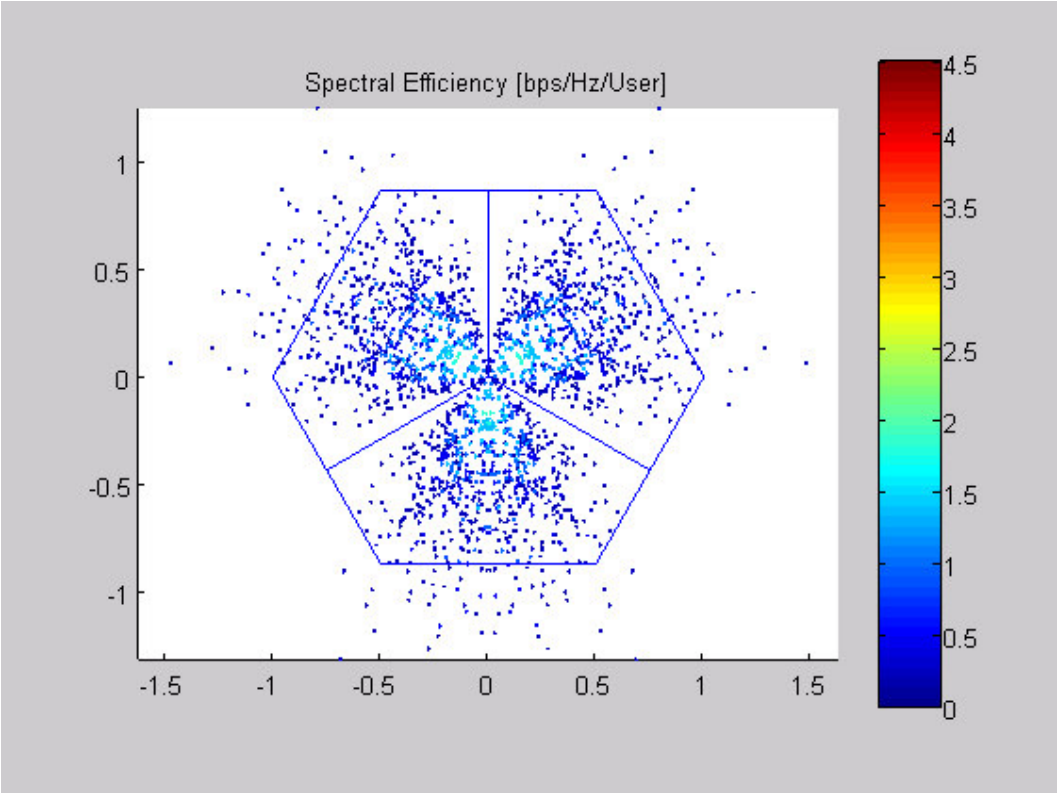

Figure 10

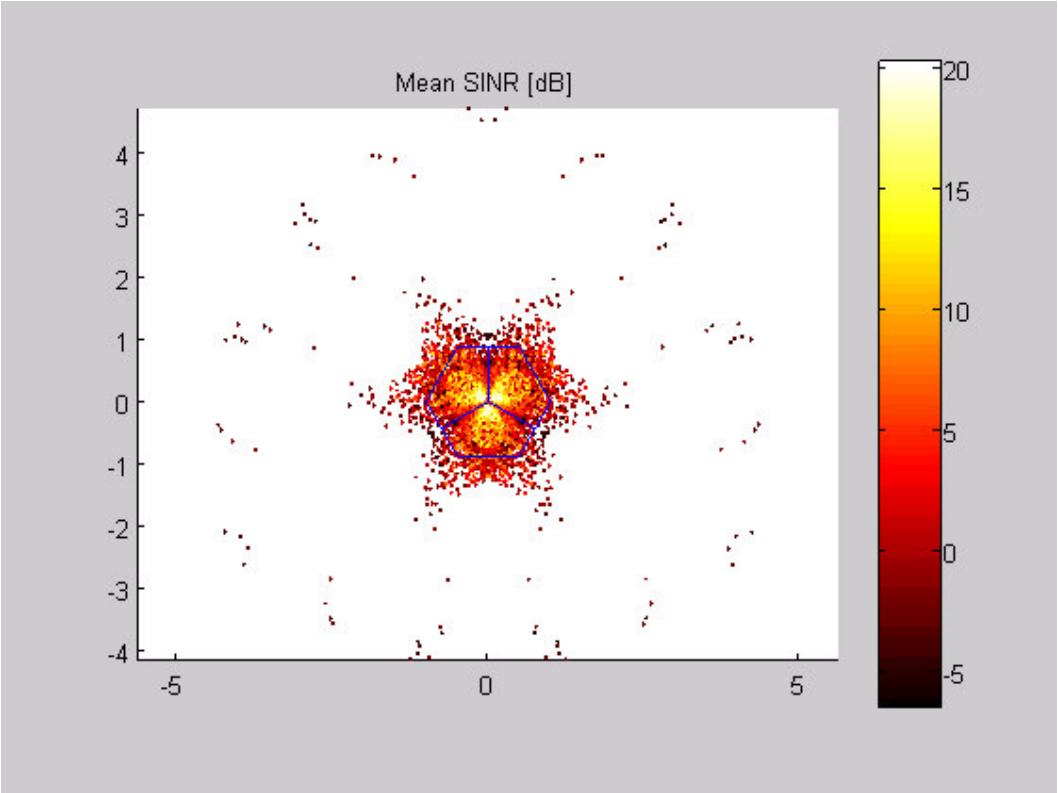

Figure 11

2.2.3.4 Ant1 reuse 3 results (K=1)

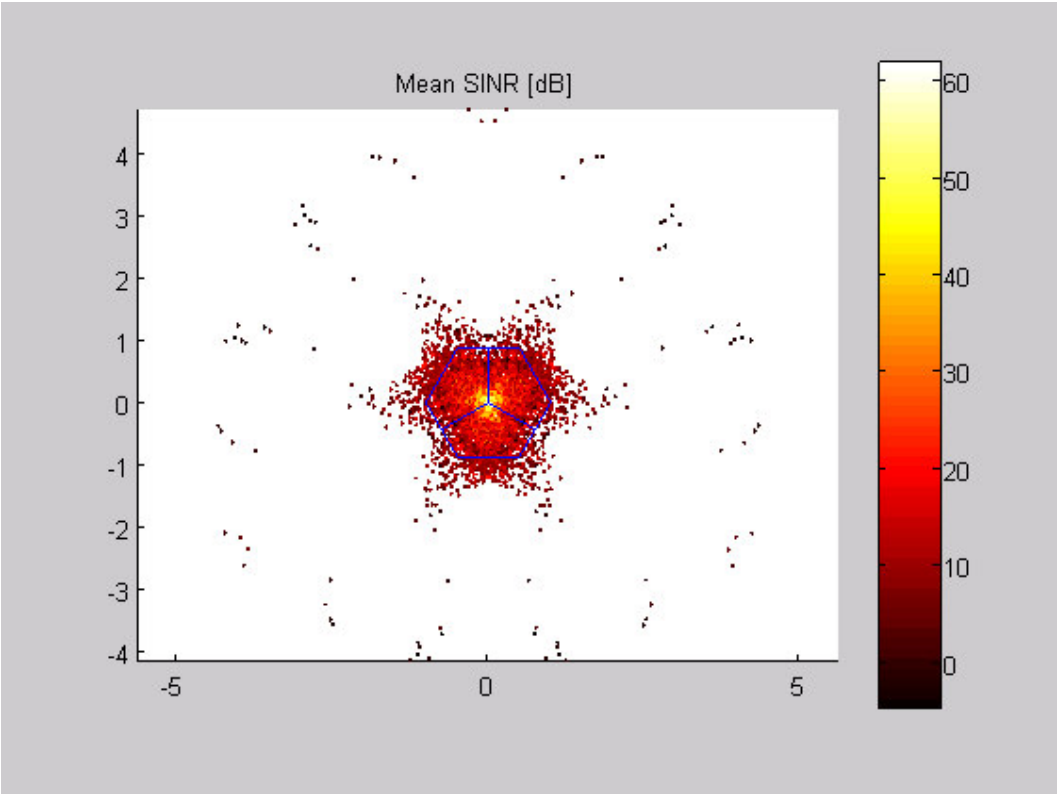

Figure 12

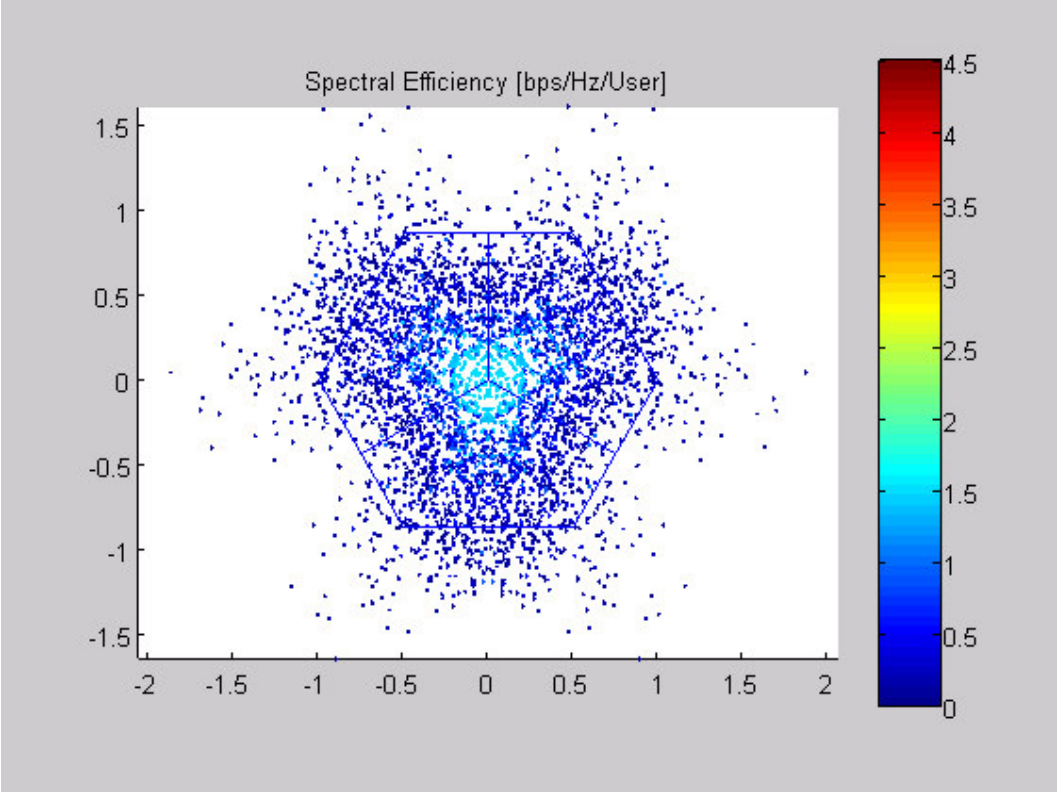
Spectral Efficiency [bps/Hz/User]
1.5
1
0.5
0
-0.5
-1
-1.5
-2
-1.5
-1
-0.5
0
0.5
1
1.5
2
4.5
4
3.5
3
2.5
2
1.5
1
0.5
0

Figure 13

2.3 Frequency diversity gain in conjunction with beamforming

Permutations in which subcarriers are adjacent or piecewise-adjacent are particularly useful for AAS use, because the continuity in the frequency domain allows for improved channel estimation, a critical feature for AAS operation. AMC and the tile structures that exist in [6] (such as the uplink PUSC and optional PUSC) are examples of such structures.

AMC transmissions occur, by design, over a *single* contiguous frequency band and thus provide no frequency diversity. This feature allows the MAC layer to select, for each SS, the optimal frequency band for operation. This scheme was shown to provide a significant performance advantage. However for this scheme to operate, the channel needs to remain relatively static over periods of time equivalent to the MAC layer latency and processing time. In medium to high vehicular velocities, the MAC layer will not accommodate the fast channel variations.

It can be argued that other modes, such as the downlink PUSC and FUSC modes provide ample frequency diversity. However, these modes are less suitable for AAS operation since training signals are shared among all the subchannels. As a consequence, beamforming cannot be done separately for each subchannel, but rather for each major group in downlink PUSC mode, and over the entire bandwidth in FUSC mode.

Another argument that can be made is that spatial diversity, typically provided in AAS systems, compensates for the lack of frequency diversity. In the next subsection it is shown that even when spatial diversity is present, frequency diversity can significantly reduce the required fade margin.

The solution we propose contains more pilot overhead compared to other downlink structures that are defined [6]. These additional pilots are especially important in a mobile AAS environment, where the AAS preambles are of limited use due to large channel variations over time.

2.4 The importance of frequency diversity

In this section we analyze interaction of frequency diversity and spatial diversity.
In the following we shall use the notation suggested in [4]. Consider the system described in Figure 14. The BS is located at the origin of the coordinate system. The BS consists of two antennas located at x=±d/2. The SS is located at a distance D from the BS. The line joining the SS with the BS makes an angle Φ_0 with the x-axis. The SS is surrounded by a scattering region of radius σ_s. A precise definition of σ_s will be provided later on. Note that σ_s is not restricted to be smaller than D, and the scattering region may encompass the BS.

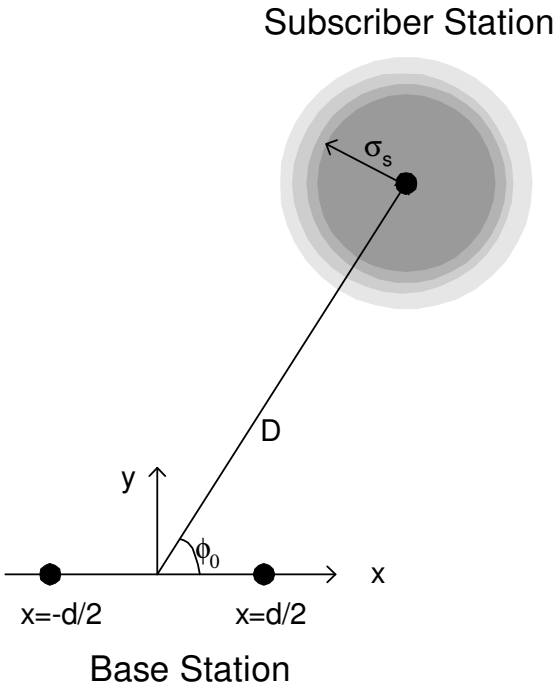

Figure 14 System model

Let $P_{AS}(\Phi)$ denote the power azimuth spectrum associated with the scattering region. The correlation between the signals received at base station antennas is given by

$$\rho_s(d) = \int \exp(jkd\cos\phi) P_{AS}(\phi) d\phi \qquad (1)$$

where $k = 2\pi/\lambda$ and λ is the wavelength of the RF carrier.

Let $P_{DS}(\tau)$ denote the delay spread spectrum associated with the scattering region. The correlation between the signal received at frequencies f_1 and f_2 is given by

$$\rho_f(\Delta f) = \frac{1}{2\pi} \int \exp(j2\pi\Delta f \cdot \tau) P_{DS}(\tau) d\tau \qquad (2)$$

with $\Delta f = f_1 - f_2$.

Next we make use of a Geometrically Based Single-Bounce (GBSB) statistical channel modeling approach (see [1] for an overview of spatial channel models) where the propagation between the SS and the BS are assumed to take place via single scattering from obstacles in the scattering region. This region is characterized by the probability density function of the scattering obstacles.
In particular we make use of a Gaussian Scattering Model (GSM). The GSM was proposed in [2] and [3]. The obstacle probability density of the GSM is given by

$$p(x_m, y_m) = \frac{1}{2\pi\sigma_s^2} \exp\left(-\frac{x_m^2 + y_m^2}{2\sigma_s^2} \right) \qquad (3)$$

Here, x_m and y_m denote the coordinate of the obstacle relative to the SS.

In [4], Janaswamy derived closed form expressions for the power azimuth spectrum (PAS) and the power delay spread spectrum (PDS) for the GSM. Using expressions for PAS and PDS, he showed agreement to the measurement results provided by Pedersen, [5].

Although close form analytical expressions exist, we have used Monte Carlo techniques to compute the spatial and frequency correlations given in (1) and (2). We used the following conditions

- Carrier frequency f_{RF} = 2.6GHz
- Frequency separation Δf=5/6 MHz.
- Spatial separation d=10 λ.
- 30 obstacles were generated fro each simulation round, 10000 simulation rounds were performed.

The value of D was varied in the range of 100m to 4km.The value of σ_s was varied from 10m to 200m. (For reference, the values found by Pederson corresponded to D=1.5Km, σ_s = 162m)

The results are shown in Figure 15 where the spatial (solid lines) and frequency (dashed lines) correlation are shown. As can be seen, for large distances, the frequency correlation depends mostly on the scattering radius. The spatial correlation depends both on the scattering radius and BS-SS distance. (Actually it depends on the ratio of the two).

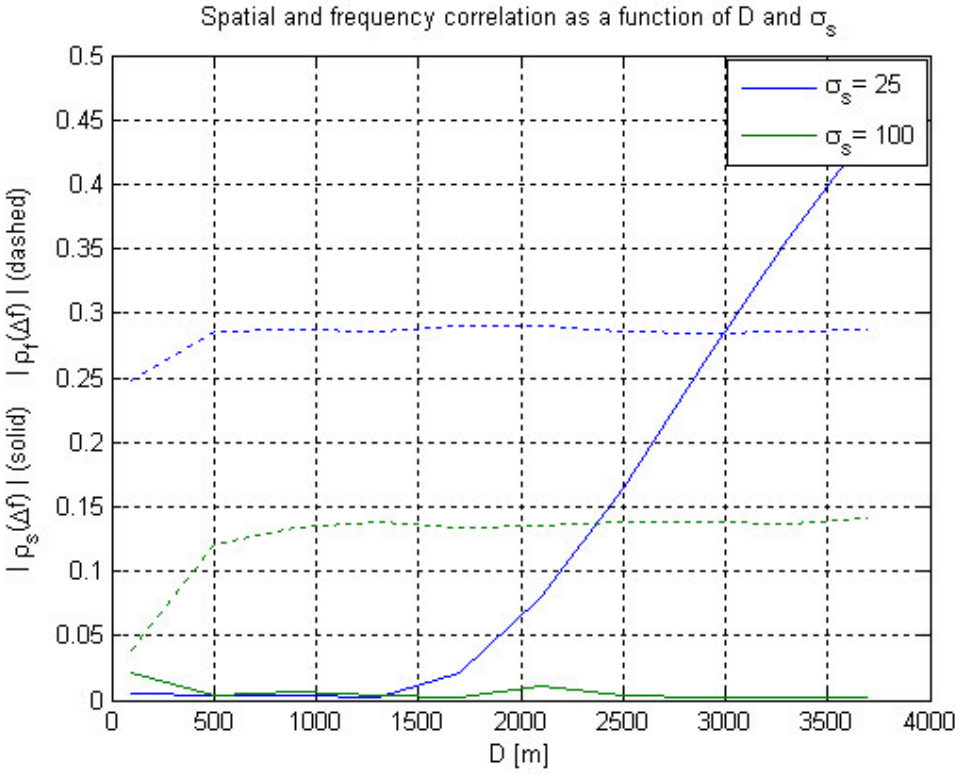

Figure 15 Spatial and frequency correlation

For large scattering radius, both correlations are low. As the scattering radius is reduced, both spatial and frequency correlations increase. For large angular spreads, (i.e. large ratios of σ_s/D), spatial correlation is lower than the frequency correlation. However for small angular spreads, frequency correlation is smaller. For the lowest angular spreads simulated, the antennas became completely correlated.

As a general conclusion, it seems that frequency diversity is important for macro-cell environment, where the distances are high and the angular spreads are small. For the microcell and picocell environments, where the angular spreads are high, spatial diversity is more important.

To evaluate the impact on system performance, we look at the required fade margin for a 1% outage probability, for the case of σ_s=25m. The fade margin is computed for the case of four antennas (d=10) and 6 frequencies (Δf=5/6 MHz). The results are shown in Figure 16. For this simulation, 50000 trials were run.

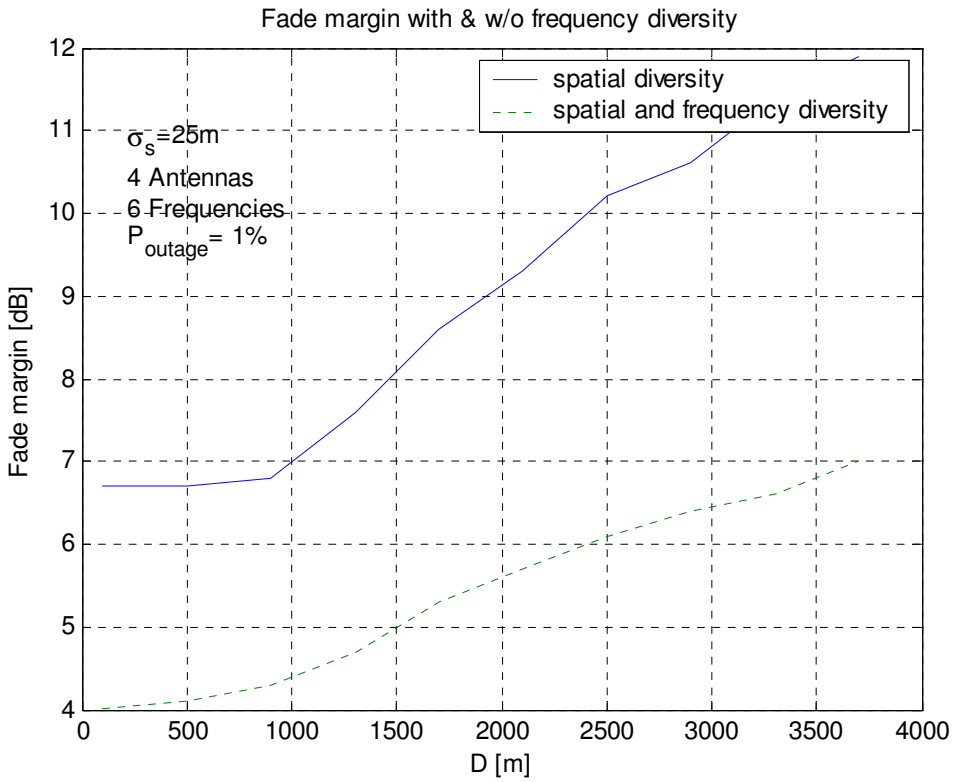

Figure 16 Fade margin

In the case of high angular spreads (low D), frequency diversity provides a reduction in fade margin of 2.5-3dB. In this case the antennas are uncorrelated, and frequency diversity increases diversity order to about 24. When D is increased the antennas become more correlated but the response across frequencies remains uncorrelated. The effective diversity order is reduced to an order of 6. In this case the improvement in fade margin is about 5dB.

Finally we look at the case of σ_s=100m. The antenna spacing and frequency spacing remain the same (10λ and Δf=5/6MHz respectively). In this case, the spatial correlation remains low even at high D. Nevertheless, the improvement in diversity due to frequency diversity is about 4 dB.

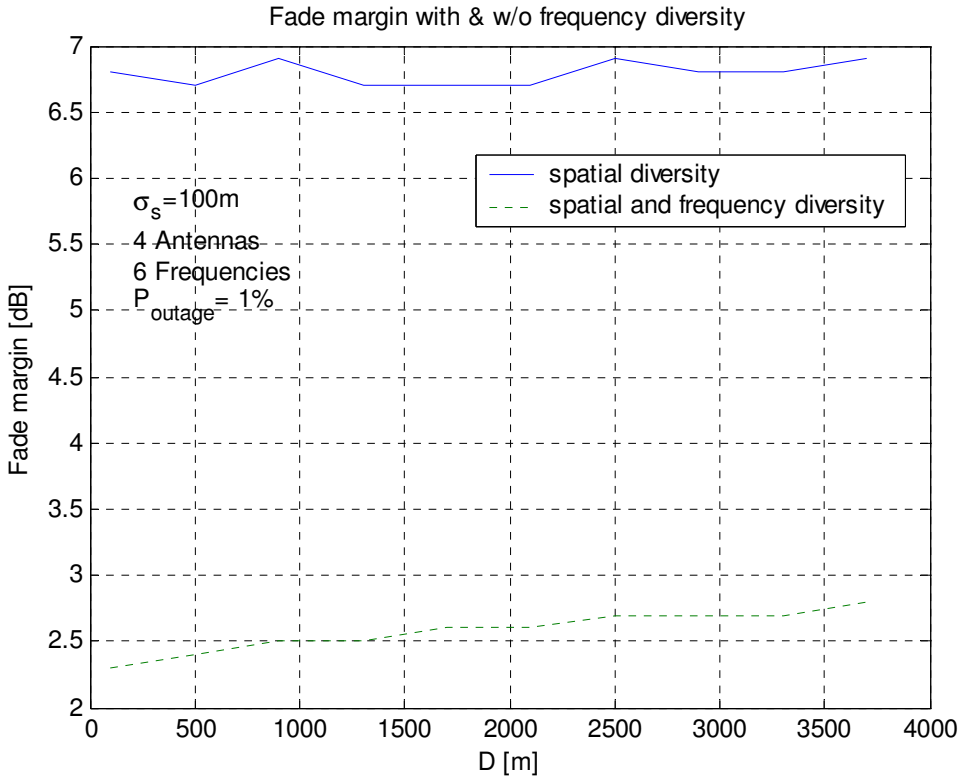

2.5 Fade Margin

In order to gain some additional insight and to provide further validation for the results of the previous section, we now calculate the fade margin for a given outage probability and for several diversity orders.

Consider a system receiving N uncorrelated signals $x_i(t)$, $i=1..N$, with total mean power of P_{ave}. The signals may originate from multiple uncorrelated antenna elements and/or from uncorrelated frequency bands. The instantaneous power of the combined received signal $y(t)$ is

$$P = |y(t)|^2 = \sum_{i=1}^{N} |x_i(t)|^2 \qquad (4)$$

For $x_i(t)$ that are Gaussian complex i.i.d., the distribution of P is χ^2 with $2N$ degrees of freedom, and the outage probability vs. fade margin can be readily obtained from the CDF of P.

Let us now examine the AMC and the uplink-PUSC permutations. A system employing the AMC permutation with M antenna elements spaced 10λ apart achieves a diversity order of M, while a system employing the UL PUSC diversity permutation with the same antenna array achieves a diversity order of $6M$, assuming that the correlation between frequencies spaced $BW/6$ apart is sufficiently low.

The following figure shows the outage probability vs. fade margin for several values of *M* with both permutations.

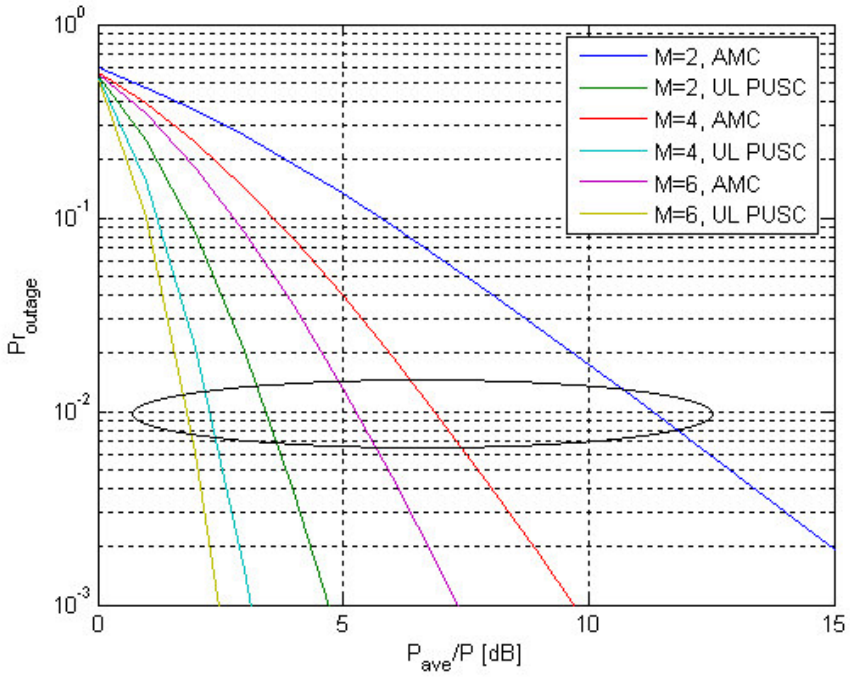

Figure 17 – Outage probability vs. fade margin. M is the number of antenna elements in the array.

The figure below shows the reduction of fade margin as a function of array size for the two permutations.

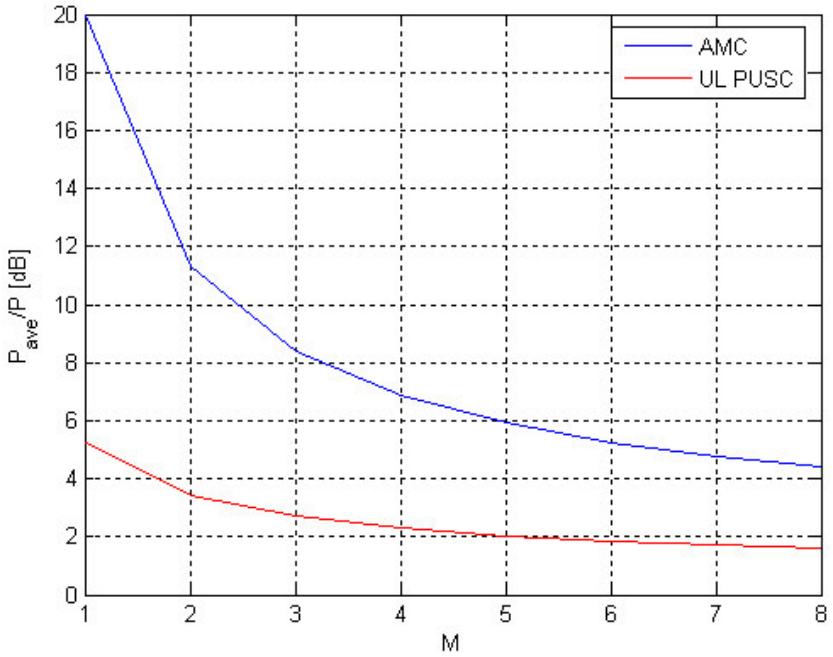

Figure 18 – Fade margin vs. number of antenna elements, for the both permutation

The fade margin of 4-4.5dB observed in the previous section is consistent with this analysis. It can be concluded that adding frequency diversity will have a positive impact on the system fade margin by an order of 4dB, in the close of 4-6 antenna elements.

3 Proposed Solution

We propose to add new permutation structures in the downlink called ‘Tile Usage of Sub-Channels’ (TUSC) and ‘Optional Tile Usage of Sub-channels’ (OTUSC). The properties of these permutations are similar to those of the uplink PUSC and OPUSC zones, except that the subchannel rotation scheme is disabled.

In order to improve the channel tracking capabilities in spatial multiplexed transmissions, the tile’s pilots may be divided between SSs. This is achieved through extensions to the already defined physical modifier IEs and MIMO DL IEs.

4 Detailed Text Changes

1. *[Modify section 8.4.3.1, page 498 lines 38-48 as follows]*

-------- BEGIN --------

• For downlink FUSC using the distributed subcarrier permutation (defined in 8.4.6.1.2.2 and 8.4.6.1.2.2.2), one slot is one subchannel by one OFDMA symbol.
• For downlink PUSC using the distributed subcarrier permutation (defined in 8.4.6.1.2.1), one slot is one subchannel by two OFDMA symbols.
• For uplink PUSC using either of the ~~distrubuted~~ distributed subcarrier permutations (defined in 8.4.6.2.1 and 8.4.6.2.5), and for downlink TUSC and OTUSC (defined in sections 8.4.6.1.2.4 and 8.4.6.1.2.5), one slot is one subchannel by three OFDMA symbols.
• For uplink and downlink using the adjacent subcarrier permutation (defined in 8.4.6.3), one slot is one subchannel by one OFDMA symbol.

-------- END --------

2. *[Modify section 8.4.4.2, page 502 lines 48-52]*

-------- BEGIN --------

The OFDMA frame may include multiple zones (such as PUSC, FUSC, PUSC with all subchannels, optional FUSC, AMC, ~~and~~ optional FUSC with all subchannels, TUSC, and OTUSC), the transition between zones is indicated in the DL-Map by the Zone_switch IE (see 8.4.5.3.4). No DL-MAP or UL-MAP allocations can span over multiple zones. Figure 219 depict OFDMA frame with multiple zones.

-------- END --------

3. *[Modify table 276 in section 8.4.5.3.3]*

-------- BEGIN --------

Table 276—OFDMA downlink AAS IE

Syntax	Size	Notes
AAS_DL_IE() {		
Extended DIUC	4 bits	AAS = 0x02
Length	4 bits	Length = 0x03
Permutation	2 bits	0b00 = PUSC permutation 0b01 = FUSC permutation 0b10 = Optional FUSC permutation 0b11 = adjacent-subcarrier permutation / other permutation (see 'other permutation select' field)
Preamble indication	2 bits	0b00 = No preamble 0b01 = Preamble used 0b10-0b11 = *Reserved*
First bin index	6 bits	When Permutation=0b10, this indicates the index of the first band allocated to this AMC segment
Last bin index	6 bits	When Permutation=0b10, this indicates the index of the last band allocated to this AMC segment

If (length = 0x04) {		
Other permutation select	2 bits	0b00 = AMC 0b01 = TUSC 0b10 = OTUSC 0b11 = *Reserved* Applicable when Permutation = 0b11
Reserved	6 bits	
}		
}		

-------- END --------

4. ***[Change 'Preamble Time Shift Index' entries in table 284 (section 8.4.5.3.11) as follows]***

-------- BEGIN --------

If (Time index shift type == 0) {		
Preamble Time Shift Index	4 bits	For PUSC, 0 – 0 sample cyclic shift 1 – floor(*NFFT*/14) sample cyclic shift …. 13 – floor(*NFFT*/14*13) sample cyclic shift 14-15 – reserved For AMC permutation, 0 – 0 sample cyclic shift 1 – floor(*NFFT*/9) sample cyclic shift …. 8 – floor(*NFFT*/9*8) sample cyclic shift 9-15 – reserved For TUSC permutation, 0 – 0 sample cyclic shift 1 – floor(*NFFT*/4) sample cyclic shift 2 – floor(*NFFT*/4*2) sample cyclic shift 3 – floor(*NFFT*/4*3) sample cyclic shift 4-15 – reserved For OTUSC permutation, 0 – 0 sample cyclic shift 1 – floor(*NFFT*/3) sample cyclic shift 2 – floor(*NFFT*/3*2) sample cyclic shift 3-15 – reserved
} else {		
Preamble Time Shift Index	4 bits	For PUSC, 0 – 0 sample cyclic shift 1 – floor(*NFFT*/14) sample cyclic shift …. 13 – floor (*NFFT*/14*13) sample cyclic shift 14-15 – reserved For AMC permutation, 0 – 0 sample cyclic shift 1 – floor (*NFFT*/9) sample cyclic shift …. 8 – floor (*NFFT*/9*8) sample cyclic shift 9-15 – reserved For TUSC permutation, 0 – 0 sample cyclic shift 1 – (*NFFT*/4) sample cyclic shift

		2 – (N_{FFT}/4*2) sample cyclic shift 3 – (N_{FFT}/4*3) sample cyclic shift 4-15 – reserved For OTUSC permutation, 0 – 0 sample cyclic shift 1 – (N_{FFT}/3) sample cyclic shift 2 – (N_{FFT}/3*2) sample cyclic shift 3-15 – reserved
}		

-------- END --------

5. ***[Add new sections 8.4.6.1.2.4, 8.4.6.1.2.4.1, 8.4.6.1.2.4.2]***

-------- BEGIN --------

8.4.6.1.2.4 Optional downlink tile usage of subchannels (TUSC)

The optional downlink TUSC is similar in structure to the uplink PUSC structure defined in section 8.4.6.2. Each transmission uses 48 data subcarriers as the minimal block of processing. The permutation properties are given in tables 311, 311b-d. The active subchannels in the TUSC zone, as defined in the DCD message (see table 356 in section 11.4.1), shall be renumbered consecutively starting from 0.

The pilots in the TUSC permutation are regarded as part of the allocation, and as such shall be beamformed in a way that is consistent with the transmission of the allocation's data subcarriers.

The TUSC permutation shall only be used within an AAS zone.

8.4.6.1.2.4.1 Symbol structure for TUSC subchannels

The TUSC symbol structure corresponds to that of the uplink PUSC structure as defined in section 8.4.6.2.1.

8.4.6.1.2.4.2 Partitioning of subcarriers into TUSC subchannels

The partitioning of subcarriers into tiles and tiles into subchannels corresponds to the definitions for the uplink PUSC structure as defined in section 8.4.6.2.2 with *UL_IDcell* replaced by *IDcell*.

-------- END --------

6. ***[Add new sections 8.4.6.1.2.5, 8.4.6.1.2.5.1, 8.4.6.1.2.5.2]***

-------- BEGIN --------

8.4.6.1.2.5 Additional optional downlink tile usage of subchannels (OTUSC)

The OTUSC is similar in structure to the uplink optional PUSC structure defined in section 8.4.6.2.5. Each transmission uses 48 data subcarriers as the minimal block of processing. The permutation properties are given in tables 313, 313a-b. The active subchannels in the OTUSC zone, as defined in the DCD message (see table 356 in section 11.4.1), shall be renumbered consecutively starting from 0.

The pilots in the OTUSC permutation are regarded as part of the allocation, and as such shall be beamformed in a way that is consistent with the transmission of the allocation's data subcarriers

The OTUSC permutation shall only be used within an AAS zone.

8.4.6.1.2.5.1 Symbol structure for OTUSC subchannels

The OTUSC symbol structure corresponds to that of the uplink optional PUSC structure as defined in section 8.4.6.2.5.1.

8.4.6.1.2.5.1 Partitioning of subcarriers into OTUSC subchannels

The partitioning of subcarriers into tiles and tiles into subchannels corresponds to the definitions for the uplink optional PUSC structure as defined in section 8.4.6.2.5.2.

-------- END --------

7. ***[Add new section 8.4.6.1.2.6]***

-------- BEGIN --------

8.4.6.1.2.6 TUSC/OTUSC support for SDMA

The pilots in an AAS zone with TUSC or OTUSC permutation are regarded as part of the allocation, and as such shall be beamformed in a way that is consistent with the transmission of the allocation's data subcarriers. In an SDMA region, the pilots of each allocation may correspond to a different pilot pattern. The pilot patterns for TUSC permutation are as depicted in figure 249, and the patterns for the OTUSC permutation are as depicted in figure 251h.

-------- END --------

8. ***[Modify 'Permutation' entry in table 311, section 8.4.6.2.7.1]***

-------- BEGIN --------

Permutation	3 ~~2~~ bits	0b000 = PUSC perm. 0b001 = FUSC perm 0b010 = Optional FUSC perm. 0b011 = Adjacent subcarrier perm. 0b100 = TUSC 0b111 = OTUSC 0b110 – 0b111 = *reserved*

-------- END --------

9. ***[Modify section 8.4.9.4.3, page 620 lines 54-57]***

-------- BEGIN --------

For the manadory tile structure in the uplink, and for the TUSC/OTUSC structures in the downlink, pilot subcarriers shall be inserted into each data burst in order to constitute the symbol and they shall be modulated according to their subcarrier location within the OFDMA symbol.

-------- END --------

10. ***[Modify section 8.4.9.4.3, page 621 lines 1-3]***

-------- BEGIN --------

In the downlink, except for the TUSC structure, and for the optional uplink tile structure each pilot shall be transmitted with a boosting of 2.5 dB over the average power of each data tone. The Pilot subcarriers shall be modulated according to the following formula:

-------- END --------

11. ***[Add the following entries to the end of table 356a ('DCD channel encoding') in section 11.4.1]***

-------- BEGIN --------

Name	Type	Length	Value	PHY scope
TUSC permutation active subchannels bitmap	XXX	9	This is a bitmap describing the sub-channels allocated to the segment in the DL, when using the TUSC permutation (see 8.4.6.1.2.4). The LSB of the first byte shall correspond to subchannel 0. For any bit that is not set, the SS on that segment shall not use the corresponding subchannel. The active subchannels are renumbered consecutively starting from 0.	OFDMA
OTUSC permutation active subchannels bitmap	XXX	13	This is a bitmap describing the sub-channels allocated to the segment in the DL, when using the OTUSC permutation (see 8.4.6.1.2.5). The LSB of the first byte shall correspond to subchannel 0. For any bit that is not set, the SS on that segment shall not use the corresponding subchannel. The active subchannels are renumbered consecutively starting from 0.	OFDMA

-------- END --------

12. ***[Modify table in section 11.8.3.7.5]***

-------- BEGIN --------

Type	Length	Value	Scope
154	1	Bit# 0: Optional PUSC support Bit# 1: Optional FUSC support Bit# 2: AMC support Bit# 3: TUSC support Bit# 4: OTUSC support Bits# ~~3~~5–7: Reserved, shall be set to zero	SBC-REQ (see 6.3.2.3.23) SBC-RSP (see 6.3.2.3.24)

-------- END --------

13. ***[Modify table in section 11.8.3.7.X adopted in contribution C80216e-05_084r4]***

11.8.3.7.X SDMA Pilot capability

Type	Length	Value	Scope
YYY	1	Bit #0-#1: SDMA pilot pattern support for AMC zone: 0b00 – no support 0b01 – support SDMA pilot patterns #A and #B 0b11 – support all SDMA pilot patterns 0b10 – reserved Bit #2: SDMA pilot pattern support for TUSC/OTUSC zone. Bits #~~2~~3 -#7: Reserved	SBC-REQ SBC-RSP

5 Acknowledgement

The authors would like to acknowledge Dr. Jack Cohen for his assistance in preparing the analysis and simulation in section 2.4.

6 References

[1] R. B. Ertel, P. Cardieri, K. W. Sowerby, T. S. Rappaport and J. H. Reed, *"Overview of Spatial Channel Models for Antenna Array Communication Systems"*, IEEE Personal Communications • February 1998 pp 10-22,

[2] J. Fuhl, A. F. Molisch, and E. Bonek, "Unified channel model for mobile radio systems with smart antennas," IEE Proc. Radar, Sonar, Navig., vol. 145, pp. 32–41, Feb. 1998.

[3] C. Ward, M. Smith, A. Jeffries, D. Adams, and J. Hudson, "Characterizing radio propagation channel for smart antenna systems," Electron. Commun. Eng. J., pp. 191–201, Aug. 1996.

[4] R. Janaswamy, "Angle and Time of Arrival Statistics for the Gaussian Scatter density Model " IEEE TRANSACTIONS ON WIRELESS COMMUNICATIONS, VOL. 1, NO. 3, JULY 2002, pp 488-497

[5] K. I. Pedersen, P. E. Mogensen, and B. H. Fleury, , "A stochastic model of the temporal and azimuthal dispersion seen at the base station in outdoor propagation environments," IEEE Trans. Veh. Technol., vol. 49, pp. 437–447, Mar. 2000.

[6] IEEE P802.16-2004.

[7] 3GPP TR 25.996

[8] "OFDM EESM simulation Results for System-Level Performance Evaluations, and Text Proposal for Section A. 4.5 of TR 25.892", Nortel Networks, R1-04-0089, 3GPP TSG-RAN-1/TSG-RAN-4 Ad Hoc, January 2004

[9] "Full verification of the EESM for OFDM in realistic interference scenarios", Huawei, R1-04-0558, 3GPP TSG RAN WG1 #37, May 2004

[10] "New results on realistic OFDM interference", Huawei, R1-04-0189, 3GPP TSG RAN WG1 #36, February 2004